in color when compared with controls. At 6 weeks, small spots of normal color had appeared on a yellowish background. These normal-colored areas expanded and had largely replaced the liver at 12 weeks after birth.

Histologically, both control and *Albumin-Cre;Dicer1*$^{loxP/loxP}$ mouse livers showed homogeneous appearance at 3 weeks of age, even though hepatocytes of *Albumin-Cre;Dicer1*$^{loxP/loxP}$ mice showed abnormalities at cytologic levels as described later (Supplementary Figure 1). At 6 weeks after birth, *Albumin-Cre;Dicer1*$^{loxP/loxP}$ mouse livers displayed round nodules consisting of enlarged but otherwise normal hepatocytes. The nodules of normal-appearing hepatocytes further expanded and largely replaced the parenchyma of 12-week-old *Albumin-Cre;Dicer1*$^{loxP/loxP}$ mouse livers.

We suspected that these progressive morphologic changes represented the replacement of *Dicer1*-decifient hepatocytes with wild-type hepatocytes that had escaped Cre-mediated recombination. To test this hypothesis, we examined the expression of the *Cre* transgene and *Dicer1*. Quantitative PCR analysis revealed the widespread silencing of *Cre* expression and a concomitant recovery of *Dicer1* expression between 6 and 12 weeks after birth (Figure 1*B* and 1*C*). Because Dicer is essential for the maturation of microRNAs, we also examined the expression of mir-122, a hepatocyte-specific microRNA. Mir-122 expression was almost completely diminished at 3 weeks but was reestablished in older mice, indicating the recovery of proper microRNA processing (Figure 1*D*). In situ hybridization showed the extensive loss of mir-122 expression in 3-week-old *Albumin-Cre;Dicer1*$^{loxP/loxP}$ mouse livers, ensuring the efficient disruption of *Dicer1* at this stage (Figure 1*E*). However, at 6 weeks of age, we observed the appearance of mir-122–positive hepatocyte nodules that corresponded to normal-colored spots observed on gross examination.

These findings indicate that *Dicer1* allele is efficiently disrupted at 3 weeks in *Albumin-Cre;Dicer1*$^{loxP/loxP}$ mouse livers; however, the entire liver is gradually repopulated by *Dicer1*-positive hepatocytes over time, and this process is achieved by nodular growth of *Dicer1*-positive wild-type hepatocytes. We did not observe oval/stem cell marker expression, including cytokeratin 19, CD34, and A6 antigen, in *Dicer1*-positive hepatocyte nodules during this process (data not shown), suggesting that liver progenitor cells do not contribute to the repopulation process.

We also assessed microRNA expression in 3-week-old *Albumin-Cre;Dicer1*$^{loxP/loxP}$ mouse livers using microarray (Figure 1*F*). The analysis identified 45 microRNAs down-regulated more than 2-fold with a false discovery rate <0.05 in *Dicer1*-deficient livers (Supplementary Tables 2 and 3). Remarkably, all 4 previously reported liver-specific microRNAs (mir-122, -148a, -192, and -194) showed robust down-regulation in *Dicer1*-deficient livers.[15] There were 9 microRNAs up-regulated in *Dicer1*-deficient livers; they are likely expressed by nonparenchymal cells and reflect secondary effects.

Dicer1-*Deficient Hepatocytes Exhibit Increased Proliferative Activity and Overwhelming Apoptosis*

Immunohistochemistry for phospho-histone H3 revealed a modest increase in hepatocyte proliferation in 3-week-old *Albumin-Cre;Dicer1*$^{loxP/loxP}$ mouse livers (Figure 2*A* and 2*B*). At the same time, *Dicer1*-deficient hepatocytes showed increased apoptosis as indicated by staining for cleaved caspase-3 (Figure 2*A* and 2*C*). Examination of 6-week-old *Albumin-Cre;Dicer1*$^{loxP/loxP}$ mouse livers revealed that both *Dicer1*-deficient hepatocytes and *Dicer1*-positive hepatocytes located in expanding nodules showed a similar increase in proliferation. In contrast, wild-type mouse livers displayed very low proliferative activity at this stage (Figure 2*D* and 2*E*). However, there was a marked difference in their apoptotic activity; apoptosis was almost exclusively observed in *Dicer1*-deficient hepatocytes (Figure 2*D* and 2*F*). These findings indicate that loss of *Dicer1* in hepatocytes causes an increase in hepatocyte proliferation. Nonetheless, most of the mutant cells are lost to elevated apoptosis over time, allowing repopulation by wild-type hepatocytes that had escaped Cre-mediated recombination.

Loss of Dicer1 *Impairs Lipid and Glucose Metabolism*

To further address the consequences of Dicer loss, we characterized 3-week-old mice, a time point at which *Dicer1* is efficiently eliminated. Except for some alterations in lipid levels, serum analyses did not reveal significant changes that would indicate liver dysfunction (Table 1). Histologic analysis confirmed that the normal liver architecture was preserved (Figure 3*A*). However, *Dicer1*-deficient hepatocytes had small vacuoles in their cytoplasm; these vacuoles were identified as lipid droplets using electron microscopy. The prominent lipid accumulation is likely responsible for the discoloration of the mutant livers. In contrast, glycogen granules normally present in hepatocytes were barely detectable in *Dicer1*-deficient hepatocytes. These findings were confirmed using histochemical analysis; oil red O staining confirmed the presence of numerous lipid droplets, and periodic acid–Schiff staining showed the depletion of glycogen in *Dicer1*-deficient hepatocytes. A detailed analysis of the lipid composition revealed a remarkable elevation of cholesterol ester and triglyceride levels, whereas the free cholesterol and free fatty acid levels were mildly increased (Figure 3*B–E*). Our studies also revealed that the depletion of glycogen storage led to impaired blood glucose maintenance. *Albumin-Cre;Dicer1*$^{loxP/loxP}$ mice kept on normal feeding showed only a mild decrease in their glucose levels; however, the mutant mice became severely hypoglycemic after 6 hours of fasting (Figure 3*F*). Thus, Dicer

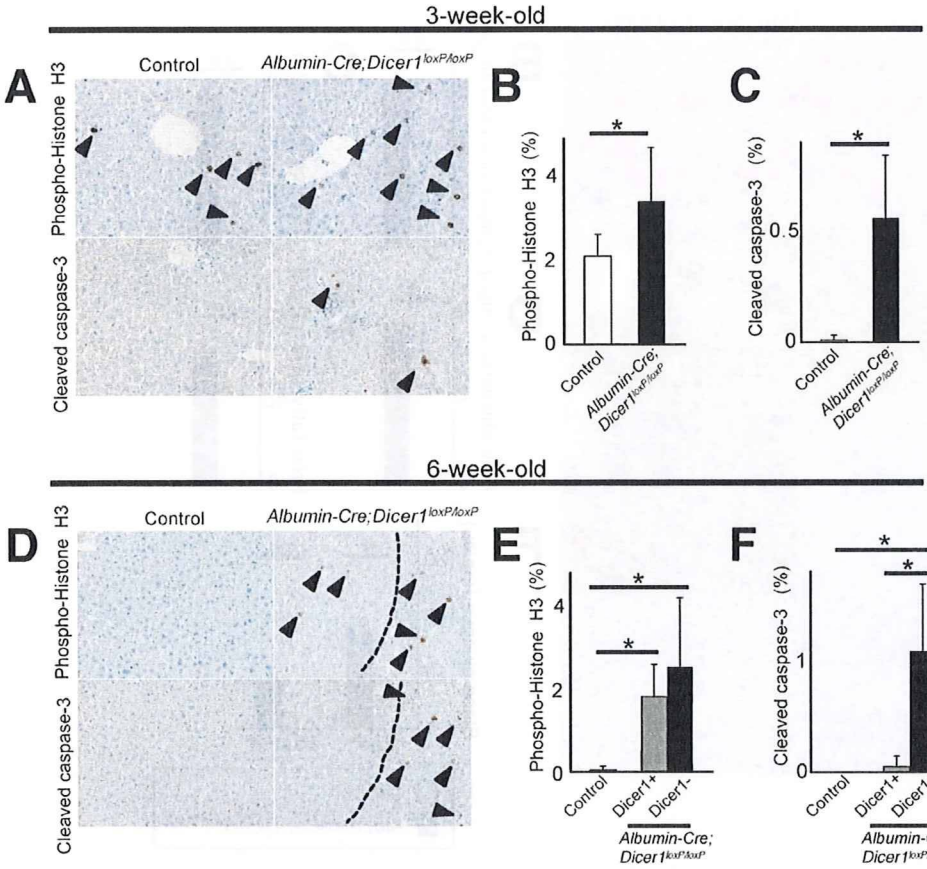

Figure 2. Increased hepatocyte proliferation and apoptosis in *Dicer1*-deficient hepatocytes. (*A* and *D*) Immunohistochemistry for phospho-histone H3 and cleaved caspase-3 in (*A*) 3-week-old and (*D*) 6-week-old mouse livers. *Dotted lines* in 6-week-old *Albumin-Cre;Dicer1*$^{loxP/loxP}$ mouse livers indicate borders between *Dicer1*-positive hepatocyte nodules (*left side*) and *Dicer1*-negative areas (*right side*). (*B*, *C*, *E*, and *F*) Quantification of hepatocyte proliferation and apoptosis in *Albumin-Cre;Dicer1*$^{loxP/loxP}$ mouse livers (n = 4–7 for each group). At least 1000 cells were counted for quantification of phospho-histone H3 and cleaved caspase-3–positive hepatocytes. For 6-week-old *Albumin-Cre;Dicer1*$^{loxP/loxP}$ *mice*, hepatocytes in *Dicer1*-positive (*gray columns*) and *Dicer1*-negative (*black columns*) areas were separately examined. $^{*}P < .05$.

function is critical for the regulation of liver lipid and glucose metabolism.

We also examined changes in the nonparenchymal cell population. Sinusoidal endothelial cells and portal tracts, including bile ducts, were not significantly altered (Supplementary Figure 2*A*). Some hematopoietic cell colonization was observed in *Dicer1*-deficient livers, and the presence of megakaryocytes and erythroblasts was confirmed by immunohistochemistry (Supplementary Figure 2*B*). In contrast, hematopoietic cells are completely absent at 3 weeks of age in control littermates. While the liver is a place for hematopoiesis during fetal stages, the liver normally loses the capacity to support hematopoiesis around the perinatal stage. The persistent presence of hematopoietic cells may represent an immature differentiation state of *Dicer1*-deficient liver.

Table 1. Metabolic Measurements of 3-Week-Old *Albumin-Cre;Dicer1*$^{loxP/loxP}$ Mice

	Control mice	*Albumin-Cre; Dicer1*$^{loxP/loxP}$ mice	*P* value
Alanine aminotransferase (*U/L*)	40.0 ± 17.0	45.6 ± 24.8	.70
Aspartate aminotransferase (*U/L*)	104.5 ± 60.2	136.6 ± 82.8	.52
γ-Glutamyl transpeptidase (*U/L*)	3.0 ± 3.8	3.4 ± 1.5	.85
Albumin (*g/dL*)	2.7 ± 0.4	2.6 ± 0.4	.83
Total protein (*g/dL*)	4.8 ± 0.3	4.0 ± 0.9	.14
Direct bilirubin (*mg/dL*)	0.1 ± 0.1	0.1 ± 0.1	.65
Indirect bilirubin (*mg/dL*)	0.0 ± 0.0	0.2 ± 0.1	.053
Triglyceride (*mg/dL*)	46.3 ± 11.8	32.6 ± 19.0	.22
Free fatty acid (*μEq/L*)	553.8 ± 156.3	1065 ± 333.2	.023
Cholesterol ester (*mg/dL*)	56.3 ± 7.0	41.6 ± 3.4	.017
Free cholesterol (*mg/dL*)	18.3 ± 1.0	58.6 ± 13.6	.0026

NOTE. n = 4–5 for each group.

Dysregulated Expression of Fetal Stage–Specific Genes in Dicer1*-Deficient Livers*

We next sought to determine whether *Dicer1*-deficient hepatocytes retain their terminally differentiated mature phenotypes. Quantitative PCR analysis revealed that the expression of liver-enriched transcription factors was maintained, with *Onecut1* and its direct target gene *Hnf1b* up-regulated significantly in *Dicer1*-deficient livers[16] (Figure 4*A*). *Hnf1a* and *Cebpb* also showed minor changes in expression levels. To further determine the differentiation status of *Dicer1*-deficient hepatocytes, we examined the expression of a battery of developmentally regulated genes. This analysis revealed dysregulated ex-

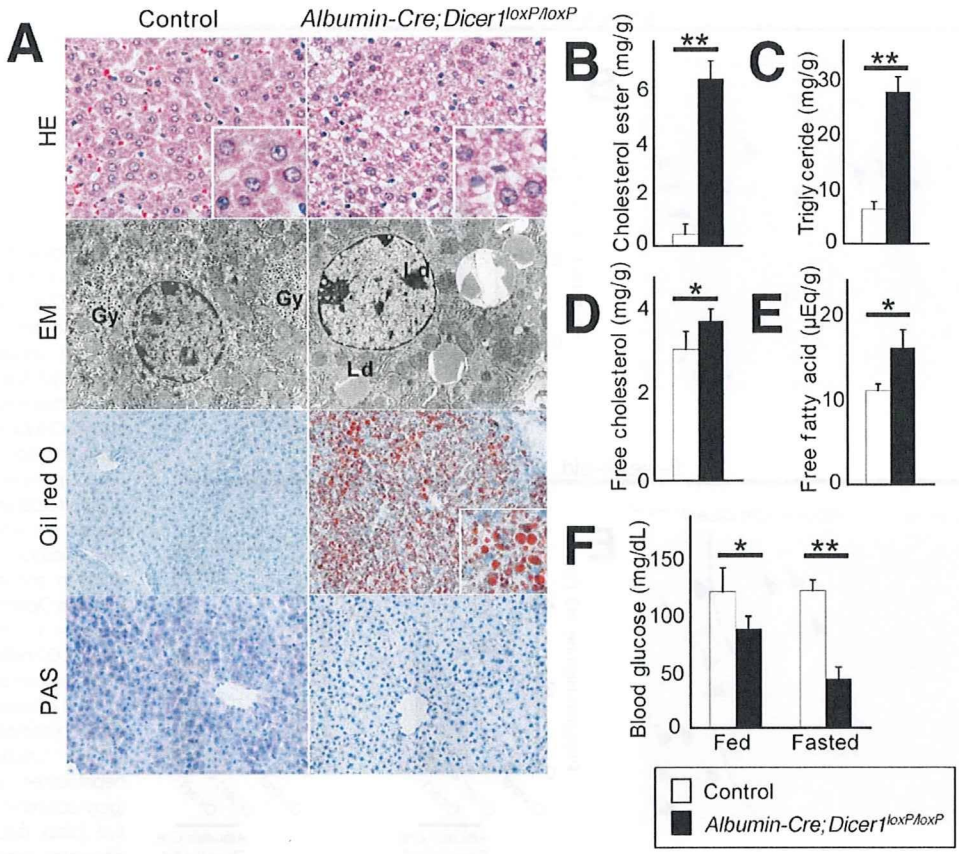

Figure 3. Impaired lipid and glucose metabolism in *Albumin-Cre;Dicer1*$^{loxP/loxP}$ mice. (*A*) Histology and ultrastructure of control and *Albumin-Cre;Dicer1*$^{loxP/loxP}$ mouse livers. Hepatocytes of control mice displayed uniform eosinophilic cytoplasm and were arranged in a trabecular pattern. The liver architecture was preserved in the *Albumin-Cre;Dicer1*$^{loxP/loxP}$ mice, but the hepatocytes exhibited small cytoplasmic vacuoles. Electron microscopy analysis of *Dicer1*-deficient hepatocytes revealed a lack of glycogen granules that are readily observed in control hepatocytes (Gy). Instead, the *Dicer1*-deficient hepatocytes contained an abundance of lipid droplets (Ld). Lipid accumulation was barely detectable in the control liver, whereas numerous lipid droplets were visible in *Dicer1*-deficient liver by oil red O staining. Periodic acid–Schiff staining highlighted glycogen in the control liver but not in the *Dicer1*-deficient liver. (*B–E*) Lipid analysis of the liver. The lipid composition of the liver tissue was determined following methanol/chloroform extraction. (*F*) Blood glucose analysis. Tail vein blood glucose level was measured in a fed condition or after 6 hours of starvation. n = 4–5 for each group. $^{*}P < .05$; $^{**}P < .0001$.

pression of genes that mark immature hepatocytes, whereas the expression pattern of genes normally found in mature hepatocytes was preserved (Figure 4*B*). The latter genes included *Sdh* and *Tdo*, which are activated during the terminal stages of liver development. Thus, with some quantitative alterations, the fundamental hepatocyte transcriptional programs of mature hepatocytes were maintained in the absence of *Dicer1*. However, Dicer function is required to repress the fetal gene expression program in adult liver.

Dicer1-*Deficient Livers Show Increased Expression of Cell Cycle–Promoting Genes and Suppression of Genes for Steroid Biosynthesis*

To define global changes in gene expression, we conducted a complementary DNA microarray analysis. The analysis generated a list of genes with more than 2-fold changes, including 1415 up-regulated and 944 down-regulated genes, that was analyzed for the enrichment in Gene Ontology categories to identify biological pathways regulated by *Dicer1*. The most enriched Gene Ontology term among the overexpressed genes was "cell division" ($P = 8.2 \times 10^{-13}$). A list of growth-promoting genes, including those encoding cyclins and aurora kinases, was found to be up-regulated in the *Dicer1*-deficient livers (Table 2). The Gene Ontology term most overrepresented among down-regulated genes was "steroid biosynthesis" ($P = 1.6 \times 10^{-15}$; Table 2). Of note, 2 previous studies using antisense oligonucleotide have shown that genes for cholesterol synthesis were down-regulated in the absence of mir-122.[4,5] In addition, we observed that previously identified direct targets of mir-122 were up-regulated modestly in *Dicer1*-deficient liver (Figure 4*C*).

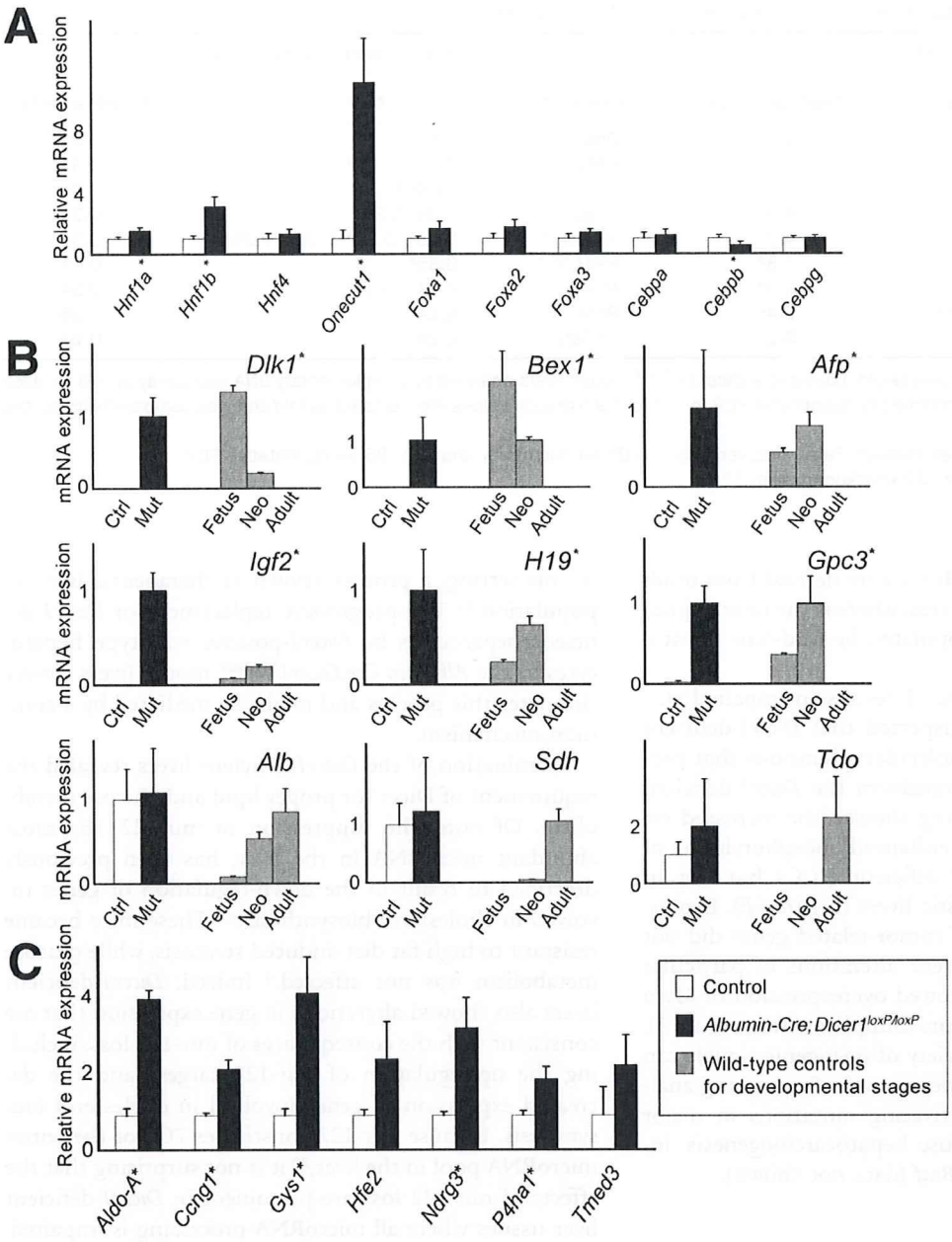

Figure 4. Expression of liver-enriched transcription factors, developmentally regulated genes, and mir-122 target genes in *Dicer1*-deficient livers. (*A*) Relative expression levels of liver-enriched transcription factors. Quantitative PCR analysis of liver samples from *Albumin-Cre;Dicer1*$^{loxP/loxP}$ and control littermates at 3 weeks after birth (n = 4 for each group). (*B*) The expression of developmentally regulated genes in control and *Albumin-Cre;Dicer1*$^{loxP/loxP}$ mice at 3 weeks (n = 5 for each group). The expression levels of wild-type mouse livers at different developmental stages were used as references (n = 3 for each group). (*C*) Expression of putative direct targets of mir-122 in *Albumin-Cre;Dicer1*$^{loxP/loxP}$ mouse livers (n = 4 for each group). Values are shown as mean ± SD. $^*P < .05$. Ctrl, control; Mut, mutant (*Albumin-Cre;Dicer1*$^{loxP/loxP}$ mice); fetus, embryonic day 14 fetus; Neo, postnatal day 0 neonate; Adult, postnatal day 42 adult.

Development of HCC in Albumin-Cre;Dicer1$^{loxP/loxP}$ *Mice*

Given that *Dicer1*-deficient hepatocytes were mostly replaced by wild-type cells at 12 weeks after birth, we were surprised to observe that one third of *Albumin-Cre;Dicer1*$^{loxP/loxP}$ mice developed HCCs after 6 months (Figure 5*A*–*C*). Furthermore, 12-month-old mice showed increased tumor incidence and progression of the disease, including 3 mice that died of tumors at 9–11 months. However, none of the mice developed metastatic lesions. Similarly to human HCCs, these tumors exhibited considerable histologic variations, including trabecular, pseudoglandular, and solid arrangements with variable degrees of steatosis (Figure 5*B*).

Remarkably, the tumors exhibited a decreased expression of *Dicer1*, persistent *Cre* transgene expression, a lack of mir-122 expression, and high expression levels of fetal liver genes (Figure 6*A*–*D*). Nonneoplastic areas consisted exclusively of histologically normal hepatocytes without evidence of preneoplastic or dysplastic changes (data not shown). In addition, nonneoplastic liver tissues obtained from tumor-bearing mice had lost *Cre* expression and were positive for *Dicer1* and mir-122 at levels comparable to those in the control littermates (Figure 6*A*–*C*). These

Table 2. Altered Gene Expression in *Albumin-Cre;Dicer1$^{loxP/loxP}$* Mouse Liver

Genes related to cell division			Genes related to steroid synthesis		
Gene name	Microarray	Quantitative PCR	Gene name	Microarray	Quantitative PCR
Aurka	2.8[a]	4.0[a]	*Dhcr7*[b]	0.30[a]	0.29[a]
Aurkb	2.2, 2.5[a]	3.5[a]	*Fdft1*[b]	0.21[a], 0.28[a]	0.37[a]
Ccna2	2.4[a], 2.6[a]	3.7[a]	*Fdps*[b]	0.066[a]	0.09[a]
Ccnb1	2.8[a], 3.0[a]	4.0[a]	*Hmgcr*	0,36, 0.39	0.29
Ccnb2	3.0[a]	4.0[a]	*Hmgcs1*[b]	0.18[a], 0.22[a], 0.22[a], 0.29[a]	0.37[a]
Ccnd1	2.8[a], 3.1[a], 3.1[a]	3.8[a]	*Hsd17b7*	0.35[a]	0.51
Ccng1[b]	2.2[a]	2.3[a]	*Mvk*[b]	0.14[a], 0.34[a]	0.34
E2f5	0.7, 1.5, 2.0[a]	2.4[a]	*Pmvk*	0.14[a]	0.25[a]
Plk1	3.6[a]	5.2[a]	*Tm7sf2*	0.28[a]	0.27[a]

NOTE. Gene expression levels of 3-week-old *Albumin-Cre;Dicer1$^{loxP/loxP}$* mouse livers analyzed by complementary DNA microarray (n = 3 for each group); the results were further confirmed by quantitative PCR (n = 4 for each group). Values are indicated as fold changes compared with control mouse livers.

[a]Genes with significantly altered expression. False discovery rate <0.05 for microarray and $P < .05$ for quantitative PCR.

[b]Significantly altered genes in mir-122 knockdown study.[4,5]

findings indicate that the HCCs were derived from residual *Dicer1*-deficient hepatocytes, whereas the nonneoplastic areas were entirely repopulated by wild-type hepatocytes.

Because disruption of *Dicer1* results in impaired survival of hepatocytes, we suspected that *Dicer1*-deficient HCCs harbor additional molecular alterations that protect from apoptosis and transform the *Dicer1*-deficient hepatocytes. Western blotting showed the increased expression of Erk1/2 and the enhanced phosphorylation of Erk1/2 and Akt in *Dicer1*-deficient HCCs but not in *Dicer1*-deficient nonneoplastic livers (Figure 6*E*). Expression analysis of a panel of tumor-related genes did not identify robust and consistent alterations of particular oncogenes in HCCs but showed overexpression of *Mycn* and *Bcl2* in a subset of tumors (Supplementary Figure 3). This may suggest that a variety of oncogenic signals can transform *Dicer1*-deficient hepatocytes. Sequencing analysis did not reveal any activating mutations in major oncogenes involved in mouse hepatocarcinogenesis, including *Ctnnb1*, *Hras*, and *Braf* (data not shown).

Discussion

Our findings indicate that the loss of *Dicer1* compromises hepatocyte survival in vivo. As indicated by the almost complete loss of mir-122, the *Alb* promoter-mediated expression of Cre recombinase in hepatocytes achieved the efficient disruption of *Dicer1* in the liver at 3 weeks after birth. However, *Dicer1*-deficient hepatocytes exhibited increased apoptosis and wild-type hepatocytes that had escaped the Cre-mediated recombination of *Dicer1* gradually repopulated the entire liver in the absence of progenitor cell expansion. Previous studies have noted that wild-type hepatocytes can display a selective growth advantage over hepatocytes with metabolic defects in vivo.[17,18] A small number of donor wild-type hepatocytes can repopulate a metabolically defective liver in this setting, a process known as therapeutic liver repopulation.[19] The progressive replacement of *Dicer1*-deficient hepatocytes by *Dicer1*-positive wild-type hepatocytes in the *Albumin-Cre;Dicer1$^{loxP/loxP}$* mouse livers closely simulates this process and might be mediated by a common mechanism.

Examination of the *Dicer1*-deficient livers revealed the requirement of Dicer for proper lipid and glucose metabolism. Of note, the suppression of mir-122, the most abundant microRNA in the liver, has been previously described to result in the down-regulation of genes involved in cholesterol biosynthesis.[4,5] These mice became resistant to high-fat diet–induced steatosis, while glucose metabolism was not affected.[4] Indeed, *Dicer1*-deficient livers also showed alterations in gene expression that are consistent with the consequences of mir-122 loss, including the up-regulation of mir-122 targets and the decreased expression of genes involved in cholesterol biosynthesis. Because mir-122 constitutes 70% of the entire microRNA pool in the liver,[20] it is not surprising that the effects of mir-122 loss are prominent in *Dicer1*-deficient liver tissues where all microRNA processing is impaired. However, in contrast to the findings obtained in the mir-122 knockdown study, the disruption of *Dicer1* resulted in marked steatosis, indicating that Dicer regulates lipid metabolism through a mir-122–dependent as well as a mir-122–independent pathway. This suggests the presence of microRNAs other than mir-122 that play critical roles in metabolic regulation in the liver. Because loss of Dicer impacts expression of a large number of genes, it is difficult to identify a specific pathway responsible for the steatosis in *Dicer1*-deficient livers. Further studies, including modulation of single microRNAs, would be required to clarify the mir-122–independent mechanisms for the regulation of lipid and glucose metabolism in the liver.

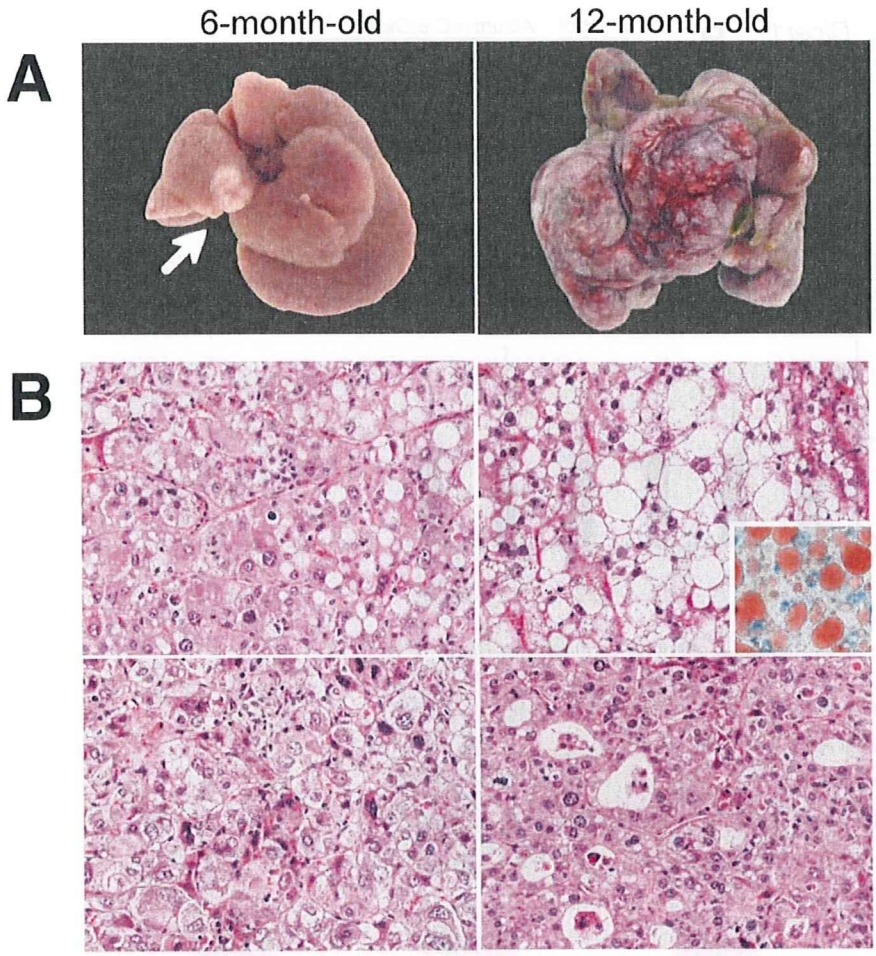

C

	6-month-old		12-month-old	
	Control	*Alb-Cre;Dicer(fl/fl)*	Control	*Alb-Cre;Dicer(fl/fl)*
Mice examined	20 M:F = 14:6	41 M:F = 12:29	19 M:F = 11:8	21 M:F = 9:12
Mice with tumors	0	15 (36.5%) M:F = 7:8	0	14 (66.7%) M:F = 6:8
Tumor size		2-20mm Average 5.5mm		2-25mm
Tumor number		1-5 Average 1.76		1-numerous

Figure 5. Development of HCC in *Albumin-Cre;Dicer1$^{loxP/loxP}$* mice. (*A*) HCCs in *Albumin-Cre;Dicer1$^{loxP/loxP}$* mice at 6 and 12 months after birth. A single tumor was observed in a 6-month-old *Albumin-Cre;Dicer1$^{loxP/loxP}$* mouse liver (*left*, *arrow*). A 12-month-old *Albumin-Cre;Dicer1$^{loxP/loxP}$* mouse liver carried multiple tumors that had replaced the liver parenchyma (*right*). (*B*) Histologic spectrum of HCCs included thick trabecular arrangement with mild steatosis (*top*, *left*), prominent steatosis (*top*, *right*) as highlighted by oil red O staining (*inset*), poorly differentiated tumors with a solid growth pattern (*bottom*, *left*), and a pseudoglandular pattern (*bottom*, *right*). (*C*) Summary of tumor incidence in *Albumin-Cre;Dicer1$^{loxP/loxP}$* mice. Note that 12-month-old mice with tumors include 3 mice that died from HCCs at 9–11 months of age.

Recent studies have established that microRNAs are frequently deregulated in many types of cancers, including HCCs.[21,22] Some evidence suggests that the dominant role of microRNA processing during transformation may be tumor suppression. Lu et al reported that microRNAs are predominantly down-regulated in human tumors, and Kumar et al showed that the simultaneous deletion of *Dicer1* and expression of activated K-ras enhances lung tumorigenesis.[21,23] The dysregulated expression of fetal liver genes in *Dicer1*-deficient hepatocytes is intriguing considering the notion that cancers mimic corresponding fetal tissue, a hypothesis that is supported by the common expression of a group of genes referred to as oncofetal genes.[24,25] The reactivation of fetal stage–specific genes is also a common finding in human HCCs. α-Fetopro-

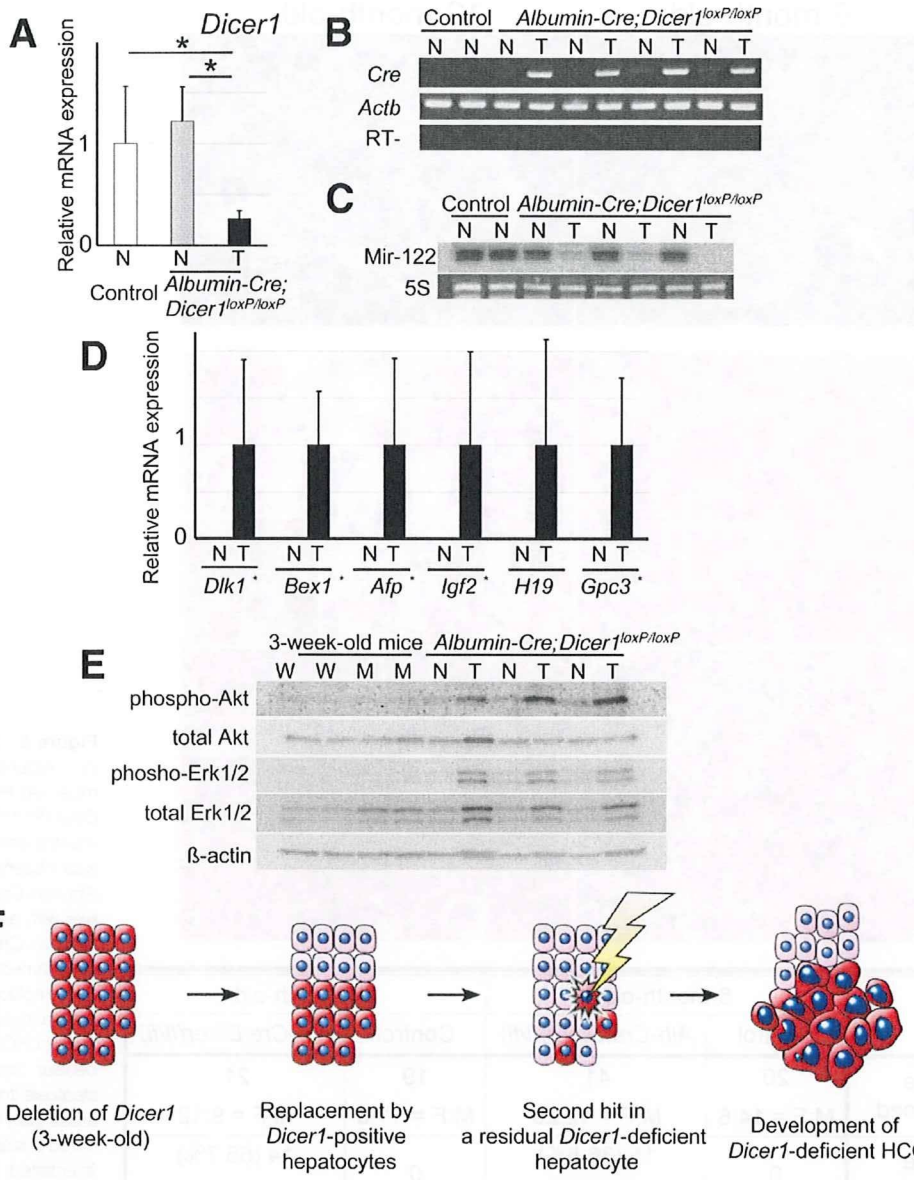

Figure 6. HCCs in *Albumin-Cre;Dicer1*$^{loxP/loxP}$ mice are derived from *Dicer1*-deficient hepatocytes. (*A*) Expression of *Dicer1* in nonneoplastic and tumor samples of control and *Albumin-Cre;Dicer1*$^{loxP/loxP}$ mice (n = 5–6 for each group). Messenger RNA expression was determined by quantitative PCR. Values are expressed as mean ± SD. $^{*}P < .05$. T, tumor; N, nonneoplastic liver tissue. (*B*) Reverse-transcription PCR analysis of *Cre* transgene expression. *Actb* served as a positive control. (*C*) Northern blot for mir-122. Ethidium bromide staining of 5S RNA served as a loading control. (*D*) Quantitative PCR analysis of oncofetal genes (n = 5–6 for each group). (*E*) Expression of phospho-Erk and phospho-Akt in HCCs and *Dicer1*-deficient livers. Protein samples from HCCs, corresponding nonneoplastic liver, and 3-week-old *Dicer1*-deficient and control livers were treated with the indicated antibodies. (*F*) Model of hepatocarcinogenesis in *Albumin-Cre;Dicer1*$^{loxP/loxP}$ mice. *Albumin-Cre;Dicer1*$^{loxP/loxP}$ mice exhibit the efficient deletion of *Dicer1* at 3 weeks after birth. However, *Dicer1*-deficient hepatocytes (*red cells*) gradually undergo apoptosis and *Dicer1*-expressing wild-type hepatocytes (*pink cells*) that have escaped Cre-mediated recombination repopulate the entire liver over time. When a *Dicer1*-deficient hepatocyte acquires secondary oncogenic stimuli presumably through additional genetic alterations, the absence of *Dicer1* cooperatively promotes the development of HCC.

tein, encoded by *AFP*, is the most widely used serum marker of HCCs in clinical practice.[26,27] Glypican-3, which is a gene product of *GPC3*, is another increasingly recognized serum and histologic marker of human HCCs.[28,29] Not only are these oncofetal genes known as tumor markers, several of their gene products, including delta-like 1, glypican-3, and insulin-like growth factor 2, have been implicated in the malignant potential of HCCs.[30–32] For instance, insulin-like growth factor 2 is a highly potent mitogen, and the

suppression of this gene alone has therapeutic benefits in a mouse implantation model of HCC.[30]

It is also notable that *Dicer1*-deficient liver showed increased expression of cell cycle–promoting genes, which is another common feature of HCCs. Even though we cannot exclude that these changes represent secondary effects such as a consequence of dysregulated fetal gene expression, it is tempting to speculate that these growth-promoting genes are controlled by a microRNA-mediated machinery. Of note, *Ccng1*, which is up-regulated also in *Dicer1*-deficient liver, has been identified as a direct target of mir-122.[4,8] Thus, *Dicer1*-deficient hepatocytes exhibit some characteristics consistent with transformed hepatocytes, including dysregulation of fetal liver genes and increased expression of cell cycle–promoting genes. However, the fact that *Dicer1*-deficient hepatocytes undergo apoptosis indicates that these changes are not sufficient to initiate tumorigenesis by themselves.

Our observations indicate that the disruption of *Dicer1* primarily impairs hepatocyte survival; however, it also promotes hepatocarcinogenesis in cells that escape the initial wave of cell death. Although these opposing effects of *Dicer1* loss on nonneoplastic hepatocytes and HCCs appear paradoxical, our findings are consistent with previous experimental observations. Impaired microRNA processing has resulted in reduced proliferative activity, tissue degeneration, or senescence in a variety of types of primary cells.[1–3,23,33–35] On the other hand, deletion of *Dicer1* promoted cellular transformation in the presence of activated K-ras both in vitro and in vivo.[23] Interestingly, it is known that the introduction of prototypical oncogenes into normal cells can induce apoptosis.[36,37] In these situations, the presence of appropriate survival signals can circumvent the apoptotic reaction and transform the cells.[37–39] Thus, the opposing effects of *Dicer1* loss on cell survival and transformation may somehow simulate those of oncogenes.

The fact that only a minor subset of *Dicer1*-deficient hepatocytes gives rise to HCCs suggests the requirement of a "second hit" that promotes hepatocarcinogenesis in *Dicer1*-deficient hepatocytes. We found that *Dicer1*-deficient HCCs consistently exhibited phosphorylation of Erk1/2 and Akt, processes that are also common in human HCCs.[40,41] Because nonneoplastic *Dicer1*-deficient livers did not show the activation of Erk1/2 or Akt, these events are not an immediate consequence of *Dicer1* loss but are acquired during tumorigenesis. Some secondary events leading to the activation of these pathways might be involved in the transformation of *Dicer1*-deficient hepatocytes and may promote hepatocarcinogenesis synergistically with the loss of *Dicer1* (Figure 6*F*).

The present study revealed novel and pivotal roles of *Dicer1* in hepatocyte survival, metabolism, developmental gene regulation, and tumor suppression in the liver. Reactivation of the fetal gene expression program might be a key mechanism of hepatocarcinogenesis induced by the loss of *Dicer1*. Because *Dicer1* is essential for microRNA processing, the phenotypes observed here would reflect the regulatory roles of microRNAs in the liver. Further studies will examine the functions of individual microRNAs to elucidate the precise mechanisms for the regulation of liver function by Dicer.

Supplementary Data

Note: To access the supplementary material accompanying this article, visit the online version of *Gastroenterology* at www.gastrojournal.org, and at doi: 10.1053/j.gastro.2009.02.067.

References

1. Harfe BD, McManus MT, Mansfield JH, et al. The RNaseIII enzyme Dicer is required for morphogenesis but not patterning of the vertebrate limb. Proc Natl Acad Sci U S A 2005;102:10898–10903.
2. Murchison EP, Partridge JF, Tam OH, et al. Characterization of Dicer-deficient murine embryonic stem cells. Proc Natl Acad Sci U S A 2005;102:12135–12140.
3. Kanellopoulou C, Muljo SA, Kung AL, et al. Dicer-deficient mouse embryonic stem cells are defective in differentiation and centromeric silencing. Genes Dev 2005;19:489–501.
4. Esau C, Davis S, Murray SF, et al. miR-122 regulation of lipid metabolism revealed by in vivo antisense targeting. Cell Metab 2006;3:87–98.
5. Krutzfeldt J, Rajewsky N, Braich R, et al. Silencing of microRNAs in vivo with 'antagomirs'. Nature 2005;438:685–689.
6. Grimm D, Streetz KL, Jopling CL, et al. Fatality in mice due to oversaturation of cellular microRNA/short hairpin RNA pathways. Nature 2006;441:537–541.
7. Ladeiro Y, Couchy G, Balabaud C, et al. MicroRNA profiling in hepatocellular tumors is associated with clinical features and oncogene/tumor suppressor gene mutations. Hepatology 2008;47:1955–1963.
8. Gramantieri L, Ferracin M, Fornari F, et al. Cyclin G1 is a target of miR-122a, a microRNA frequently down-regulated in human hepatocellular carcinoma. Cancer Res 2007;67:6092–6099.
9. Calabrese JM, Seila AC, Yeo GW, et al. RNA sequence analysis defines Dicer's role in mouse embryonic stem cells. Proc Natl Acad Sci U S A 2007;104:18097–18102.
10. Postic C, Shiota M, Niswender KD, et al. Dual roles for glucokinase in glucose homeostasis as determined by liver and pancreatic beta cell-specific gene knock-outs using Cre recombinase. J Biol Chem 1999;274:305–315.
11. Sekine S, Gutierrez P, Lan B, et al. Liver specific loss of beta-catenin results in delayed hepatocyte proliferation after partial hepatectomy. Hepatology 2007;45:361–368.
12. Obernosterer G, Martinez J, Alenius M. Locked nucleic acid-based in situ detection of microRNAs in mouse tissue sections. Nat Protoc 2007;2:1508–1514.
13. Sharov AA, Dudekula DB, Ko MS. A web-based tool for principal component and significance analysis of microarray data. Bioinformatics 2005;21:2548–2549.
14. Dennis G Jr, Sherman BT, Hosack DA, et al. DAVID: Database for Annotation, Visualization, and Integrated Discovery. Genome Biol 2003;4:P3.
15. Barad O, Meiri E, Avniel A, et al. MicroRNA expression detected by oligonucleotide microarrays: system establishment and expression profiling in human tissues. Genome Res 2004;14:2486–2494.

16. Clotman F, Lannoy VJ, Reber M, et al. The onecut transcription factor HNF6 is required for normal development of the biliary tract. Development 2002;129:1819–1828.
17. Sandgren EP, Palmiter RD, Heckel JL, et al. Complete hepatic regeneration after somatic deletion of an albumin-plasminogen activator transgene. Cell 1991;66:245–256.
18. Overturf K, Al-Dhalimy M, Tanguay R, et al. Hepatocytes corrected by gene therapy are selected in vivo in a murine model of hereditary tyrosinaemia type I. Nat Genet 1996;12:266–273.
19. Grompe M, Laconi E, Shafritz DA. Principles of therapeutic liver repopulation. Semin Liver Dis 1999;19:7–14.
20. Lagos-Quintana M, Rauhut R, Yalcin A, et al. Identification of tissue-specific microRNAs from mouse. Curr Biol 2002;12:735–739.
21. Lu J, Getz G, Miska EA, et al. MicroRNA expression profiles classify human cancers. Nature 2005;435:834–838.
22. Calin GA, Croce CM. MicroRNA signatures in human cancers. Nat Rev Cancer 2006;6:857–866.
23. Kumar MS, Lu J, Mercer KL, et al. Impaired microRNA processing enhances cellular transformation and tumorigenesis. Nat Genet 2007;39:673–677.
24. Uriel J. Cancer, retrodifferentiation, and the myth of Faust. Cancer Res 1976;36:4269–4275.
25. Alexander P. Foetal "antigens" in cancer. Nature 1972;235:137–140.
26. Taketa K. Alpha-fetoprotein: reevaluation in hepatology. Hepatology 1990;12:1420–1432.
27. Johnson PJ. The role of serum alpha-fetoprotein estimation in the diagnosis and management of hepatocellular carcinoma. Clin Liver Dis 2001;5:145–159.
28. Zhu ZW, Friess H, Wang L, et al. Enhanced glypican-3 expression differentiates the majority of hepatocellular carcinomas from benign hepatic disorders. Gut 2001;48:558–564.
29. Capurro M, Wanless IR, Sherman M, et al. Glypican-3: a novel serum and histochemical marker for hepatocellular carcinoma. Gastroenterology 2003;125:89–97.
30. Yao X, Hu JF, Daniels M, et al. A methylated oligonucleotide inhibits IGF2 expression and enhances survival in a model of hepatocellular carcinoma. J Clin Invest 2003;111:265–273.
31. Huang J, Zhang X, Zhang M, et al. Up-regulation of DLK1 as an imprinted gene could contribute to human hepatocellular carcinoma. Carcinogenesis 2007;28:1094–1103.
32. Capurro MI, Xiang YY, Lobe C, et al. Glypican-3 promotes the growth of hepatocellular carcinoma by stimulating canonical Wnt signaling. Cancer Res 2005;65:6245–6254.
33. Damiani D, Alexander JJ, O'Rourke JR, et al. Dicer inactivation leads to progressive functional and structural degeneration of the mouse retina. J Neurosci 2008;28:4878–4887.
34. Wang Y, Medvid R, Melton C, et al. DGCR8 is essential for microRNA biogenesis and silencing of embryonic stem cell self-renewal. Nat Genet 2007;39:380–385.
35. Koralov SB, Muljo SA, Galler GR, et al. Dicer ablation affects antibody diversity and cell survival in the B lymphocyte lineage. Cell 2008;132:860–874.
36. Evan GI, Wyllie AH, Gilbert CS, et al. Induction of apoptosis in fibroblasts by c-myc protein. Cell 1992;69:119–128.
37. Pelengaris S, Khan M, Evan GI. Suppression of Myc-induced apoptosis in beta cells exposes multiple oncogenic properties of Myc and triggers carcinogenic progression. Cell 2002;109:321–334.
38. Strasser A, Harris AW, Bath ML, et al. Novel primitive lymphoid tumours induced in transgenic mice by cooperation between myc and bcl-2. Nature 1990;348:331–333.
39. Jacobs JJ, Scheijen B, Voncken JW, et al. Bmi-1 collaborates with c-Myc in tumorigenesis by inhibiting c-Myc-induced apoptosis via INK4a/ARF. Genes Dev 1999;13:2678–2690.
40. Nakanishi K, Sakamoto M, Yamasaki S, et al. Akt phosphorylation is a risk factor for early disease recurrence and poor prognosis in hepatocellular carcinoma. Cancer 2005;103:307–312.
41. Schmidt CM, McKillop IH, Cahill PA, et al. Increased MAPK expression and activity in primary human hepatocellular carcinoma. Biochem Biophys Res Commun 1997;236:54–58.

Received July 9, 2008. Accepted February 19, 2009.

Reprint requests

Address requests for reprints to: Shigeki Sekine, MD, PhD, Pathology Division, National Cancer Center Research Institute, 5-1-1, Tsukiji, Chuo-ku, Tokyo, Japan. e-mail: ssekine@ncc.go.jp; fax: (81) 3-3248-2463; or Matthias Hebrok, PhD, Diabetes Center, Department of Medicine, University of California San Francisco, 613 Parnassus Avenue, HSW1112, Box 0540, San Francisco, California 94143. e-mail: mhebrok@ucsf.edu; fax: (415) 564-5813.

Acknowledgments

The authors thank Shigeru Tamura for photographic assistance, Fumio Hasegawa for electron microscopy, and John P. Morris IV for critical reading of the manuscript.

Conflicts of interest

The authors disclose no conflicts.

Funding

Supported by a Grant-in-Aid for the Third Term Comprehensive 10-Year Strategy for Cancer Control and a Grant-in-Aid for Cancer Research from the Ministry of Health, Labor and Welfare of Japan, as well as a program for promotion of Fundamental Studies in Health Sciences of the National Institute of Biomedical Innovation (NiBio), Japan. Work in M.H.'s laboratory was supported by a grant from the National Institutes of Health (CA112537).

Supplementary Table 1. Primary Antibodies Used in the Present Study

Antigen	Clone	Application	Dilution	Source
Phospho-histone H3	Polyclonal #9701	IHC-P	1:500	Cell Signaling Technology (Danvers, MA)
Cleaved caspase-3	Polyclonal #9661	IHC-P	1:500	Cell Signaling Technology
Cytokeratin 19	TROMA-III	IHC-P	1:5000	Developmental Studies Hybridoma Bank (Iowa City, IA)
TER-119	TER-119	IHC-P	1:100	BioLegend (San Diego, CA)
CD31	390	IHC-Fr	1:100	Biolegend
CD41	MWReg30	IHC-Fr	1:100	eBioscience (San Diego, CA)
ERK1/2	Polyclonal #9102	WB	1:1000	Cell Signaling Technology
Phospho-ERK1/2	Polyclonal #4377	WB	1:1000	Cell Signaling Technology
AKT	Polyclonal #9272	WB	1:250	Cell Signaling Technology
Phospho-AKT	Polyclonal #9271	WB	1:250	Cell Signaling Technology
β-Actin	AC-15	WB	1:3000	Sigma-Aldrich (St. Louis, MO)

IHC-P, immunohistochemistry (paraffin); IHC-Fr, immunohistochemistry (frozen); WB, Western blotting.

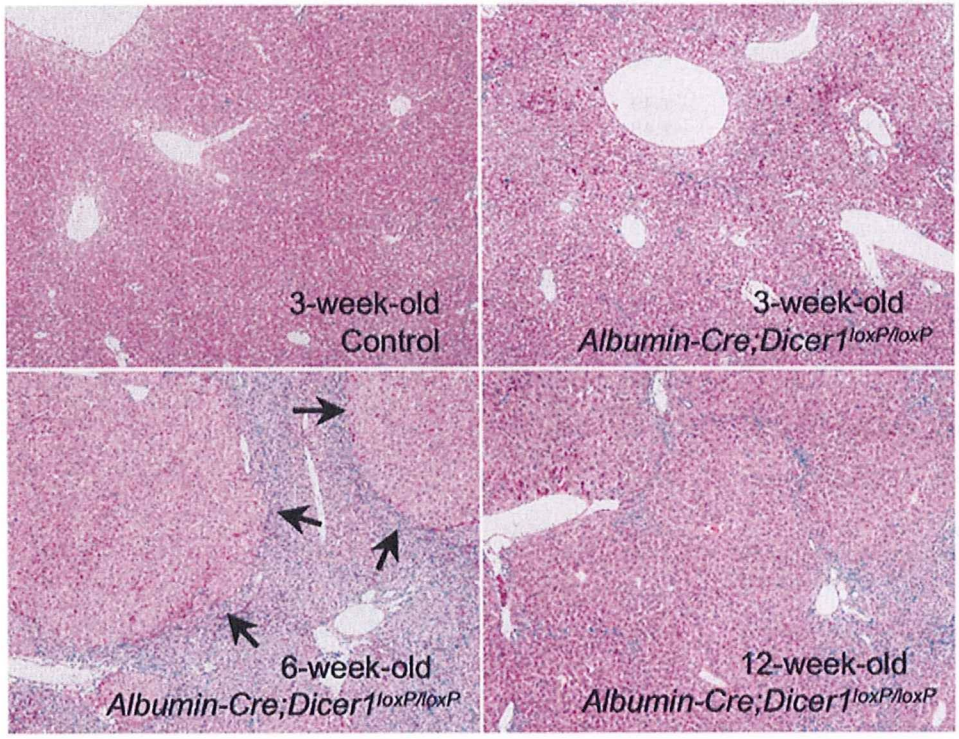

Supplementary Figure 1. Histology of control and *Albumin-Cre;Dicer1*$^{loxP/loxP}$ mouse livers during young adulthood. At 3 weeks of age, both control and *Albumin-Cre;Dicer1*$^{loxP/loxP}$ mouse livers showed homogeneous appearance, even though hepatocytes of *Albumin-Cre;Dicer1*$^{loxP/loxP}$ mice showed abnormalities at cytologic levels (see Figure 3*A* for high-magnification images). At 6 weeks after birth, *Albumin-Cre;Dicer1*$^{loxP/loxP}$ livers displayed round nodules consisting of eosinophilic and enlarged hepatocytes (*arrows*) that correspond to normal-colored areas on gross examination (Figure 1*A*) and areas positive for mir-122 expression (Figure 1*E*). Normal-appearing hepatocytes largely replaced the parenchyma of 12-week-old *Albumin-Cre;Dicer1*$^{loxP/loxP}$ livers.

Supplementary Table 2. MicroRNAs Down-regulated in *Albumin-Cre;Dicer1$^{loxP/loxP}$* Mouse Livers

Probe name	Log2 ratio	False discovery rate
hsa-miR-192/mmu-miR-192/rno-miR-192	−4.274	1.70E-05
hsa-miR-122/mmu-miR-122/rno-miR-122	−4.271	6.30E-05
hsa-miR-194/mmu-miR-194/rno-miR-194	−4.271	8.40E-06
hsa-miR-215	−4.164	1.60E-05
hsa-miR-193a-3p/mmu-miR-193/rno-miR-193	−3.822	8.40E-06
hsa-miR-122*	−3.162	2.20E-05
hsa-miR-148a/mmu-miR-148a	−3.089	8.40E-06
mmu-miR-101b/rno-miR-101b	−2.922	5.90E-05
hsa-miR-22/mmu-miR-22/rno-miR-22	−2.801	8.40E-06
hsa-miR-802/mmu-miR-802	−2.722	8.40E-06
hsa-miR-378/mmu-miR-378/rno-miR-378	−2.505	8.40E-06
hsa-miR-365/mmu-miR-365/rno-miR-365	−2.282	2.00E-05
hsa-miR-30c/mmu-miR-30c/rno-miR-30c	−2.179	2.50E-05
hsa-miR-31/mmu-miR-31/rno-miR-31	−2.113	2.00E-05
hsa-miR-101/mmu-miR-101a/rno-miR-101a	−1.944	0.00019
hsa-miR-30a/mmu-miR-30a/rno-miR-30a	−1.913	5.90E-05
hsa-miR-30e/mmu-miR-30e/rno-miR-30e	−1.764	5.50E-05
hsa-miR-30b/mmu-miR-30b/rno-miR-30b-5p	−1.674	0.00019
hsa-miR-200a/mmu-miR- 200a/rno-miR-200a	−1.617	0.00033
hsa-miR-22*/mmu-miR-22*/rno-miR-22*	−1.519	7.90E-05
hsa-miR-130a/mmu-miR-130a/rno-miR-130a	−1.508	6.60E-05
hsa-miR-200b/mmu-miR-200b/rno-miR-200b	−1.506	0.00034
hsa-miR-20a/mmu-miR-20a/rno-miR-20a	−1.49	0.00015
hsa-miR-29c/mmu-miR-29c/rno-miR-29c	−1.48	0.00018
hsa-miR-29a/mmu-miR-29a/rno-miR-29a	−1.471	0.00015
hsa-miR-19b/mmu-miR-19b/rno-miR-19b	−1.434	2.00E-04
hsa-miR-17/mmu-miR-17/rno-miR-17-5p/rno-miR-17	−1.415	0.00021
hsa-miR-106a	−1.401	0.00024
hsa-let-7f/mmu-let-7f/rno-let-7f	−1.277	0.00021
hsa-let-7a/mmu-let-7a/rno-let-7a	−1.25	0.00015
hsa-miR-30d/mmu-miR-30d/rno-miR-30d	−1.247	0.00016
mmu-let-7g	−1.241	0.00019
mmu-let-7f/rno-let-7f	−1.204	2.00E-04
mmu-let-7d/rno-let-7d	−1.167	0.00021
hsa-miR-107/mmu-miR-107/rno-miR-107	−1.163	0.00027
mmu-let-7a/rno-let-7a	−1.142	0.00021
hsa-miR-30e*/mmu-miR-30e*/rno-miR-30e*	−1.114	0.00027
hsa-let-7d/mmu-let-7d/rno-let-7d	−1.113	0.00034
hsa-miR-19a/mmu-miR-19a/rno-miR-19a	−1.107	0.0015
hsa-miR-185/mmu-miR-185/rno-miR-185	−1.088	0.00045
mmu-miR-20b	−1.087	0.00034
hsa-miR-26b/mmu-miR-26b/rno-miR-26b	−1.054	0.00028
hsa-miR-93/mmu-miR-93/rno-miR-93	−1.034	0.0011
rno-miR-352	−1.031	0.00034
hsa-miR-191/mmu-miR-191/rno-miR-191	−1.005	0.00034

NOTE. Probes that showed more than 2-fold changes with a false discovery rate <0.05 are listed.

Supplementary Table 3. MicroRNAs Up-regulated in *Albumin-Cre;Dicer1$^{loxP/loxP}$* Mouse Livers

Probe name	Log2 ratio	False discovery rate
mmu-miR-327	2.327	0.00019
mmu-miR-434-3p/rno-miR-434	1.589	0.0011
hsa-miR-142-3p/mmu-miR-142- 3p/rno-miR-142-3p	1.522	0.0011
hsa-miR-142-5p/mmu-miR-142 -5p/rno-miR-142-5p	1.321	0.00037
hsa-miR-199a-3p/hsa-miR-199b-3p/mmu-miR-199a-3p/mmu-miR-199b/rno-miR-199a-3p	1.162	0.00034
mmu-miR-434-5p	1.153	0.0035
hsa-miR-199a-5p/mmu-miR-199a-5p/rno-miR-199a-5p	1.15	0.0029
mmu-miR-199b*	1.104	0.002
hsa-miR-223/mmu-miR-223/rno-miR-223	1.057	0.00034

NOTE. Probes that showed more than 2-fold changes with a false discovery rate <0.05 are listed.

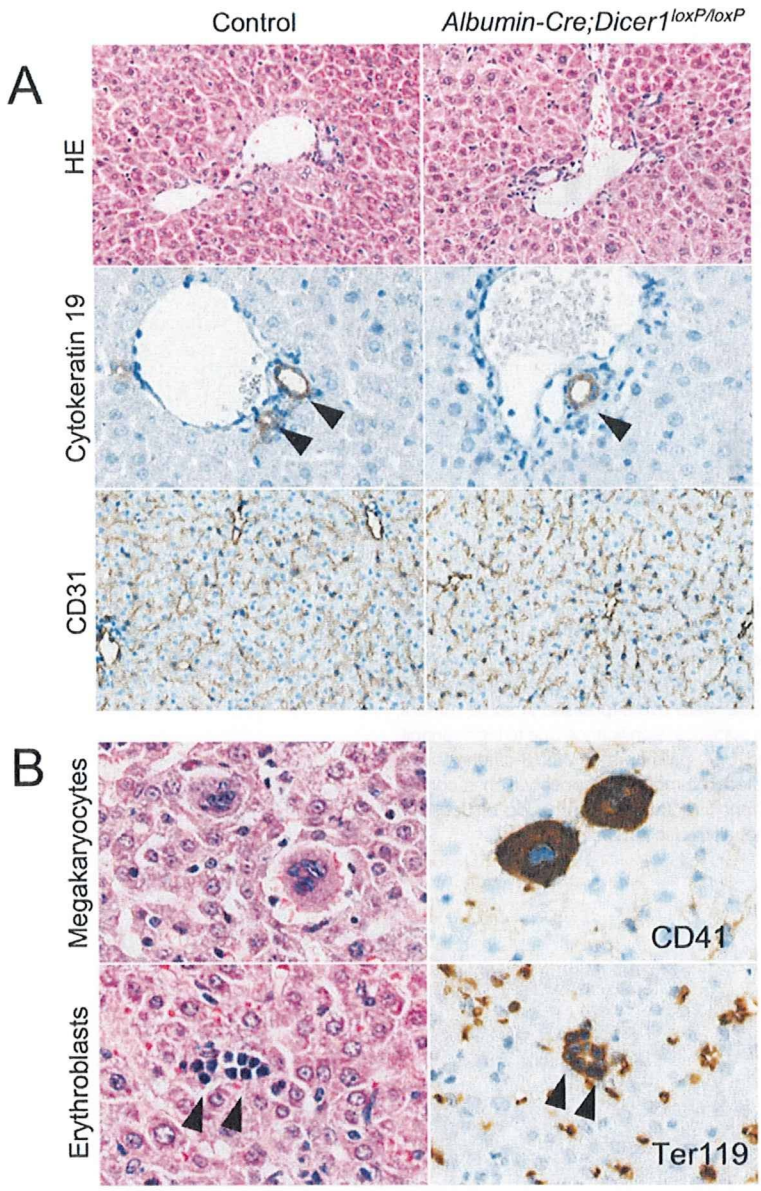

Supplementary Figure 2. Nonparenchymal cell components of *Albumin-Cre;Dicer1*$^{loxP/loxP}$ mouse livers. (*A*) Histologically, *Albumin-Cre;Dicer1*$^{loxP/loxP}$ mouse livers did not show significant alterations in portal tract morphology. Staining for cytokeratin 19 to stain bile ducts and CD31 to highlight endothelial cells did not reveal significant abnormalities. (*B*) Hematopoietic cell colonization, which is not observed in controls, was found in most *Albumin-Cre;Dicer1*$^{loxP/loxP}$ mouse livers. The presence of megakaryocytes was confirmed by staining for CD41. Islands of erythroblasts were also noted (*arrowheads*). Ter119 was positive in both erythroblasts and mature erythrocytes, but immature erythroblasts were distinguished by the presence of nuclei (*arrowheads*).

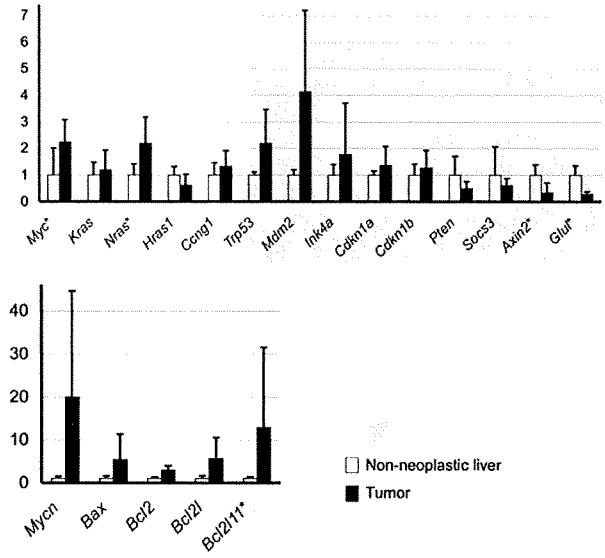

Supplementary Figure 3. Expression of tumor-related genes in *Dicer1*-deficient HCCs. Quantitative PCR analysis of nonneoplastic liver samples and HCCs from *Albumin-Cre;Dicer1*$^{loxP/loxP}$ (n = 6–8 for each group). Values are expressed as mean ± SD. $^{*}P < .05$. Two oncogenes, *Myc* and *Nras*, were significantly but only modestly up-regulated in HCCs. While *Mycn* and *Bcl2* were overexpressed in some tumors, the differences did not reach statistical significance due to high variability. Expression of *Axin2* and *Glul*, hallmarks of Wnt/β-catenin signal activation, was down-regulated in tumors. This observation is consistent with the absence of *Ctnnb1* mutations. Expression of *Socs3*, a major target of Stat3, was not altered in HCCs.

Journal of Pathology
J Pathol 2009; **219**: 365–372
Published online 27 July 2009 in Wiley InterScience
(www.interscience.wiley.com) **DOI:** 10.1002/path.2606

Original Paper

Dicer is required for proper liver zonation

Shigeki Sekine,[1]* Reiko Ogawa,[1] Michael T Mcmanus,[2] Yae Kanai[1] and Matthias Hebrok[2]
[1] *Pathology Division, National Cancer Center Research Institute, Tokyo, Japan*
[2] *Diabetes Center, Department of Medicine, University of California San Francisco, San Francisco, California, USA*

**Correspondence to: Shigeki Sekine, Pathology Division, National Cancer Center Research Institute, 5-1-1, Tsukiji, Chuo-ku, Tokyo, Japan. E-mail: ssekine@ncc.go.jp*

No conflicts of interest were declared.

Received: 21 June 2009
Revised: 17 July 2009
Accepted: 17 July 2009

Abstract

A number of genes and their protein products are expressed within the liver lobules in a region-specific manner and confer heterogeneous metabolic properties to hepatocytes; this phenomenon is known as 'metabolic zonation'. To elucidate the roles of Dicer, an endoribonuclease III type enzyme required for microRNA biogenesis, in the establishment of liver zonation, we examined the distribution of proteins exhibiting pericentral or periportal localization in hepatocyte-specific *Dicer1* knockout mouse livers. Immunohistochemistry showed that the localization of pericentral proteins was mostly preserved in *Dicer1*-deficient livers. However, glutamine synthetase, whose expression is normally confined to a few layers of hepatocytes surrounding the central veins, was expressed in broader pericentral areas. Even more striking was the observation that all the periportal proteins that were examined, including phosphoenolpyruvate carboxykinase, E-cadherin, arginase 1, and carbamoyl phosphate synthetase-I, lost their localized expression patterns and were diffusely expressed throughout the entire lobule. Thus, with regard to periportal protein expression, the consequences of Dicer loss were similar to those caused by the disruption of β-catenin. An analysis of livers deficient in β-catenin did not identify the down-regulation of *Dicer1* or any microRNAs, indicating that they are not directly activated by β-catenin. Thus, the present study illustrates that Dicer plays a pivotal role in the establishment of liver zonation. Dicer is essential for the suppression of periportal proteins by Wnt/β-catenin/TCF signalling, albeit it likely acts in an indirect manner.

Keywords: Dicer; β-catenin; liver; zonation

Introduction

Although hepatocytes are uniform at a histological level, they differ in a number of metabolic functions [1,2]. For example, pericentral hepatocytes are active in glutamine and bile acid synthesis and the metabolism of xenobiotics, whereas periportal hepatocytes are more active in cholesterol, urea, and glucose synthesis [1,2]. The metabolic heterogeneity of hepatocytes enables multiple and occasionally antagonistic metabolic functions to be performed efficiently in the liver. A number of genes and their protein products involved in these metabolic processes are expressed in a region-specific manner along the porto-central axis within the liver lobule and their respective functions confer the heterogeneous metabolic properties of hepatocytes [1–3].

Recent studies have revealed that the Wnt signalling pathway plays a key role in the establishment of liver zonation [4,5]. The Wnt signalling pathway is activated by the binding of secreted Wnt ligands to Frz and Lrp receptors on cell membranes. This leads to the stabilization of β-catenin through the inhibition of proteosomal degradation, and the translocation of the protein to the nucleus, where it activates TCF-dependent transcription [6]. β-Catenin/TCF-dependent transcription is normally active in the pericentral hepatocytes, where it induces pericentral gene expression while suppressing periportal gene expression [4,7]. The hepatocyte-specific ablation of Apc, leading to the constitutive activation of β-catenin/TCF-dependent transcription, resulted in the diffuse expression of pericentral genes and the down-regulation of periportal genes throughout the entire liver lobule [4,8]. Conversely, the suppression of Wnt signalling by the overexpression of Dkk1 or the conditional ablation of β-catenin caused a loss of pericentral gene expression and the diffuse expression of periportal genes [4,9]. Braeuning *et al* further showed that activation of the Ras/MAPK pathway by the oncogenic form of H-ras or serum components suppressed pericentral genes and induced periportal genes through the inhibition of β-catenin/TCF-dependent transcription [10,11]. Thus, the expression of pericentral and periportal genes is coordinately and inversely regulated by Wnt/β-catenin/TCF signalling.

Dicer is an essential component of microRNA biogenesis that cleaves pre-microRNAs into mature microRNAs. Since Dicer is encoded by a single locus in the mouse genome, the disruption of the single *Dicer1* gene results in the loss of virtually all microRNAs [12–14]. Here, we demonstrate that Dicer plays an essential role in the establishment of proper liver zonation. Remarkably, the loss of Dicer impairs the localization of periportal proteins, leaving the expression of pericentral proteins mostly intact. Thus, our results reveal the novel finding that microRNAs appear to be specifically required for the suppression of periportal protein expression.

Materials and methods

Mice

Alb-Cre [15,16], *Dicer1*$^{flox/flox}$ [12], *Ctnnb1*$^{flox/flox}$ [17], *Alb-Cre;Ctnnb1*$^{flox/flox}$ [7,9], and *Alb-Cre; Dicer*$^{flox/flox}$ [18] mice have been previously described. The mice used in the present study were maintained in barrier facilities and all studies were conducted in compliance with the University of California IACUC (Institutional Animal Care and Use Committee) guidelines and according to protocols approved by the Committee for Ethics in Animal Experimentation at the National Cancer Center, Japan.

Immunohistochemistry

Liver tissue samples were fixed with 10% buffered formalin, embedded in paraffin, and cut into 5-μm-thick sections. Immunohistochemistry was performed by an indirect immunoperoxidase method using peroxidise-labelled anti-mouse, -rabbit or -goat polymers (Histofine Simple Stain, Nichirei, Tokyo, Japan). 3,3′-Diaminobenzidine tetrahydrochloride was used as a chromogen. The primary antibodies that were used are listed in Table 1. For double immunofluorescence staining, anti-mouse IgG antibody conjugated with Alexa Fluor 488 and anti-rabbit IgG antibody conjugated with Alexa Fluor 594 were used as secondary antibodies. The sections were analysed using a confocal microscope (LSM5 Pascal; Carl Zeiss Jena GmbH, Jena, Germany) equipped with a 15 mW Kr/Ar laser.

Quantitative PCR

RNA extraction and the reverse-transcription reaction were performed using standard protocols. Quantitative PCR reactions were performed using SYBR Green PCR master mix (Applied Biosystems, CA, USA). The expression of *Dicer1* was compared with the expression level of *Gusb*, as previously described [9]. The primer sequences were as follows: *Dicer1*: GAACGAAATGCAAGGAATGGA and GGGACTTCGATATCCTCTTCTTTCTC; *Gusb*: ACGGGATTGTGGTCATCGA and TCGTTGCCAAAACTCTGAGGTA.

Microarray analysis

RNA samples were prepared from liver tissues of 6-week-old female *Alb-Cre;Ctnnb1*$^{flox/flox}$ and *Ctnnb1*$^{flox/flox}$ mice. The samples were labelled with a miRNA Labeling Reagent & Hybridization Kit (Agilent Technologies, CA, USA) based on the manufacturer's instructions. The labelled RNA samples were hybridized with a mouse miRNA microarray (Agilent Technologies) containing 566 mouse miRNA probes based on Sanger miRBase v10.0. MicroRNAs that showed more than two-fold changes with $p < 0.05$ (Welch t-test) were considered significant.

Results

Localization of pericentral proteins is only marginally affected in Dicer mutant mice

To elucidate the roles of Dicer in liver zonation, liver samples from *Alb-Cre;Dicer*$^{flox/flox}$ mice and their control littermates (*Dicer*$^{flox/flox}$) were immunohistochemically examined. As previously reported, the efficient deletion of *Dicer1* in hepatocytes was achieved in 3-week-old *Alb-Cre;Dicer*$^{flox/flox}$ mice; however, *Dicer1*-deficient hepatocytes were prone to apoptosis and the complete disruption of *Dicer1* was followed by repopulation with *Dicer1*-expressing hepatocytes that had escaped Cre-mediated recombination [18]. We therefore examined the livers from 3-week-old *Alb-Cre;Dicer*$^{flox/flox}$ and *Dicer*$^{flox/flox}$ mice (hereafter referred to as Dicer-deficient and control livers).

Immunohistochemistry showed that the localization of pericentral proteins was mostly maintained

Table 1. Antibodies used for immunohistochemistry

Antigen	Clone	Dilution	Source
Glutamine synthetase	6	1:1000	Becton Dickinson, Franklin Lakes, USA
GLT-1	Polyclonal	1:500	Dr Masahiko Watanabe [24]
OAT	Polyclonal	1:500	Santa Cruz Biotechnologies, Santa Cruz, USA
CYP2E1	Polyclonal	1:500	Dr Magnus Ingelman-Sundberg [25]
E-cadherin	36	1:250	Becton Dickinson, Franklin Lakes, USA
PEPCK	Polyclonal	1:200	Santa Cruz Biotechnologies, Santa Cruz, USA
CPS1	Polyclonal	1:500	Santa Cruz Biotechnologies, Santa Cruz, USA
Arginase I	19	1:2500	Becton Dickinson, Franklin Lakes, USA

OAT = ornithine aminotransferase; PEPCK = phosphoenolpyruvate carboxykinase; CPS1 = carbamoyl phosphate synthetase-I.

in the absence of Dicer. The distributions of GLT-1, ornithine aminotransferase (OAT), and CYP2E1 were unaltered in Dicer-deficient livers. GLT-1 and OAT were expressed in a few layers of hepatocytes surrounding the central veins (Figures 1A, 1B, 1D, and 1E). CYP2E1 was expressed in broader pericentral areas (Figures 1J and 1K). Expression of glutamine synthetase (GS) was observed in the pericentral areas of both mice; however, the GS-positive areas were significantly broader in the Dicer-deficient livers (Figures 1G and 1H).

The altered localization of GS was confirmed by double immunofluorescence staining for GS and CYP2E1. In control mouse livers, distinct distributions of these proteins were evident: GS expression was restricted to a few layers of hepatocytes surrounding the central veins, whereas CYP2E1 expression was extended to the distal pericentral

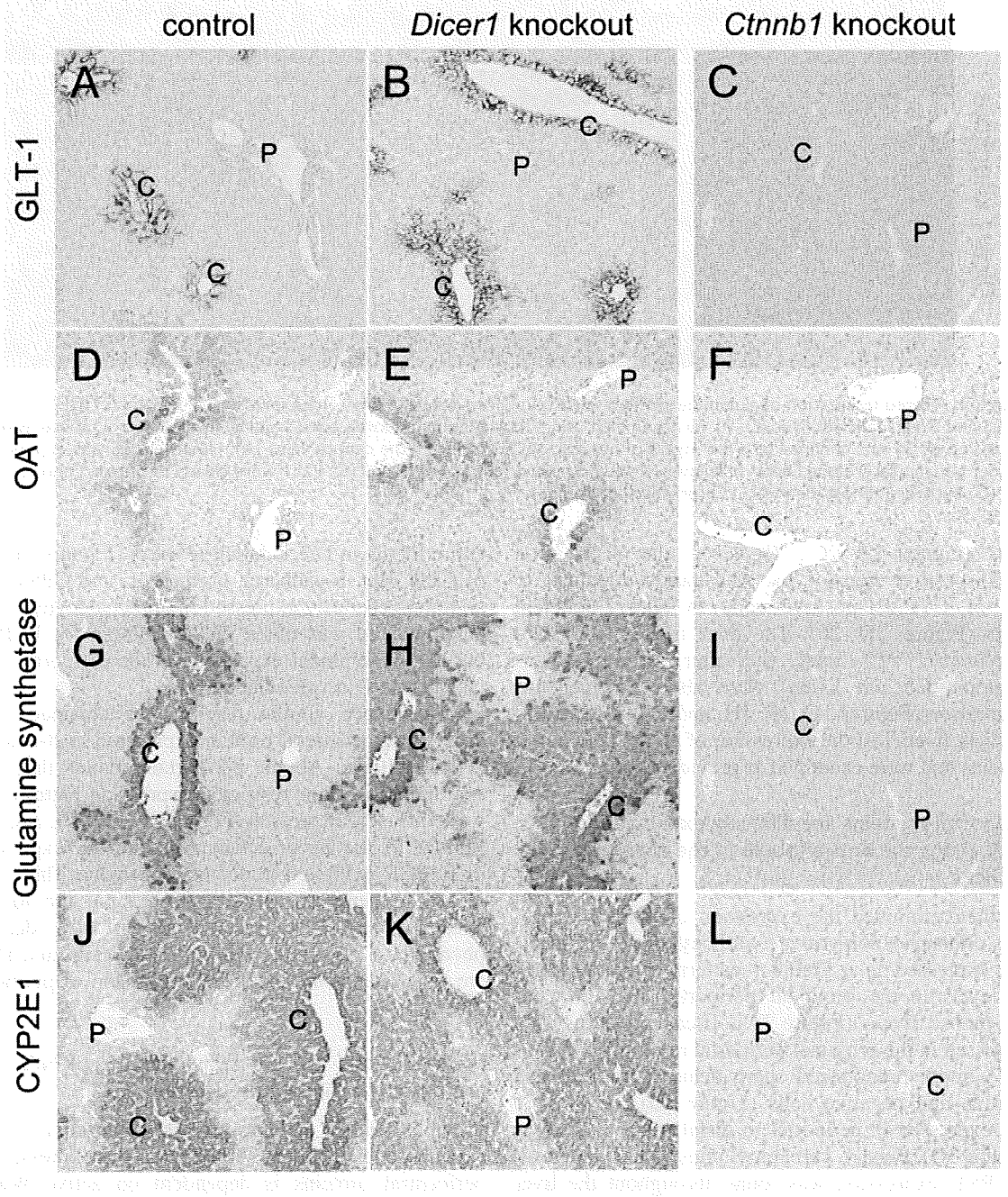

Figure 1. Expression of pericentral proteins in Dicer-deficient liver. Pericentral protein expression was examined using immunohistochemistry. The distributions of GLT-1, OAT, and CYP2E1 were unaltered in Dicer-deficient liver (B, E, K) compared with those in control mouse liver (*Dicer*$^{flox/flox}$) (A, D, J). Glutamine synthetase maintained its pericentral localization in Dicer-deficient liver (H), but its expression extended beyond its normal boundary and encompassed a broader area than that observed in control mouse liver (G). Pericentral protein expression was completely lost in β-catenin-deficient livers (C, F, I, L). C = pericentral vein; P = portal tract

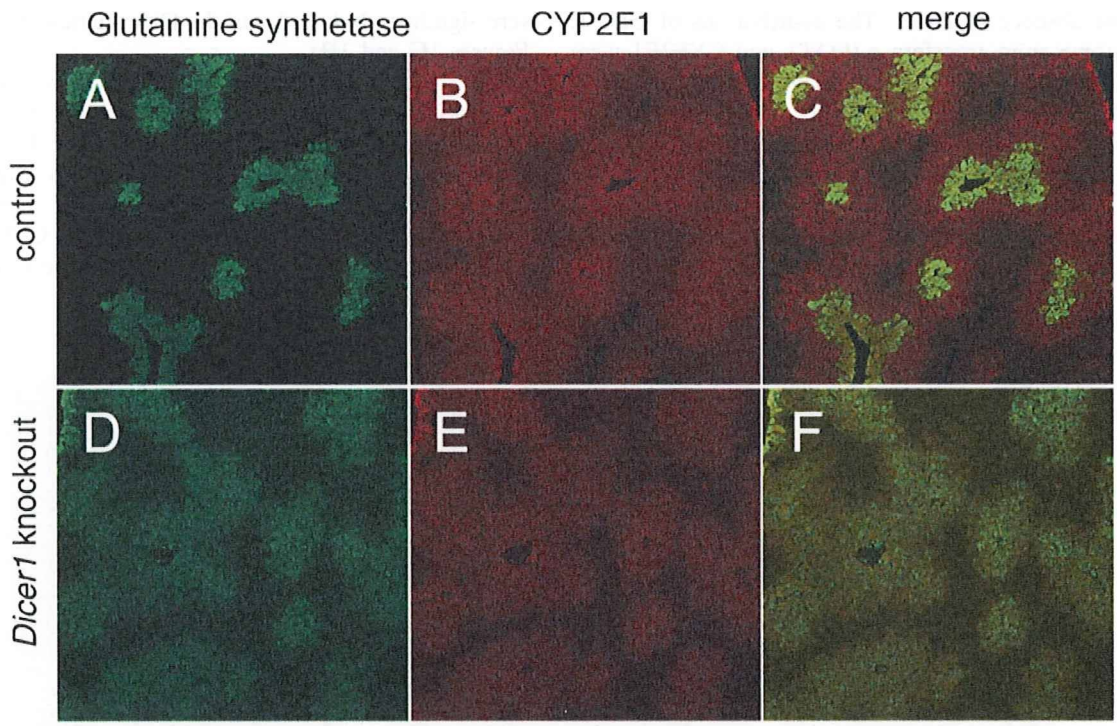

Figure 2. Altered localization of glutamine synthetase (GS) in Dicer-deficient liver. The expression of GS and CYP2E1 in control (A–C) and Dicer-deficient liver (D–F) was examined using double immunofluorescence staining. In the control mouse liver, the expression of GS was confined to a few layers of hepatocytes surrounding the central veins (A). However, GS was expressed in broader pericentral areas in Dicer-deficient livers (D). The distributions of GS and CYP2E1 were clearly distinct in control mouse liver (C) but were almost identical in Dicer-deficient liver (F)

areas (Figures 2A–2C). However, the distribution of GS-positive hepatocytes was almost identical to that of CYP2E1-positive cells in *Dicer1*-deficient livers (Figures 2D–2F). The liver tissues from *Alb-Cre;Ctnnb1*$^{flox/flox}$ mice (hereafter referred to as β-catenin-deficient livers) were also examined for comparison (Figures 1C, 1F, 1H, and 1K). β-Catenin-deficient livers lost the expression of all the pericentral proteins that were examined as previously reported [9].

Periportal proteins are diffusely expressed throughout the entire lobule in the absence of Dicer

We then examined the expression of periportal proteins. Phosphoenolpyruvate carboxykinase (PEPCK) was expressed in a gradient pattern, with the highest levels in the proximal periportal areas in control mouse livers (Figure 3A). E-cadherin was also expressed in the proximal periportal regions but exhibited a more pronounced sharp demarcation between positive and negative cells (Figure 3D). Arginase 1 was expressed in periportal to distal pericentral areas (Figure 3G). Finally, carbamoyl phosphate synthetase-I (CPS1) expression was found throughout the liver lobules, with the exception of a few layers of perivenous hepatocytes; this distribution was complementary to that of GS (Figure 3J). Remarkably, all of these periportal proteins lost their localized expression patterns and appeared in a diffuse pattern throughout the entire lobule in Dicer-deficient livers (Figures 3B, 3E, 3H, and 3K). E-cadherin, arginase 1, and CPS1 were all homogeneously expressed in all hepatocytes. Some heterogeneity was noted in the staining for PEPCK, but the predominant expression in the periportal areas was lost in Dicer-deficient livers.

Interestingly, similar results were obtained in an analysis of periportal protein expression in β-catenin-deficient livers. All the periportal proteins that were examined lost their restricted expression patterns and were diffusely expressed (Figures 3C, 3F, 3I, and 3L). Similar to the Dicer-deficient livers, the expression of PEPCK exhibited minor heterogeneity. Thus, with regard to periportal protein expression, the loss of β-catenin and Dicer resulted in virtually identical phenotypes, suggesting that both β-catenin and Dicer are required for the localized expression of periportal proteins.

Neither *Dicer1* nor any individual microRNAs are directly activated by β-catenin/TCF

Previous studies and the present observations on β-catenin-deficient livers showed that the expression of pericentral proteins is dependent on active Wnt/β-catenin signalling [4,9]. The conserved pericentral protein expression therefore indicates that Wnt signalling is still active in the pericentral hepatocytes of Dicer-deficient livers. On the other hand, periportal proteins are diffusely expressed throughout the liver lobules in

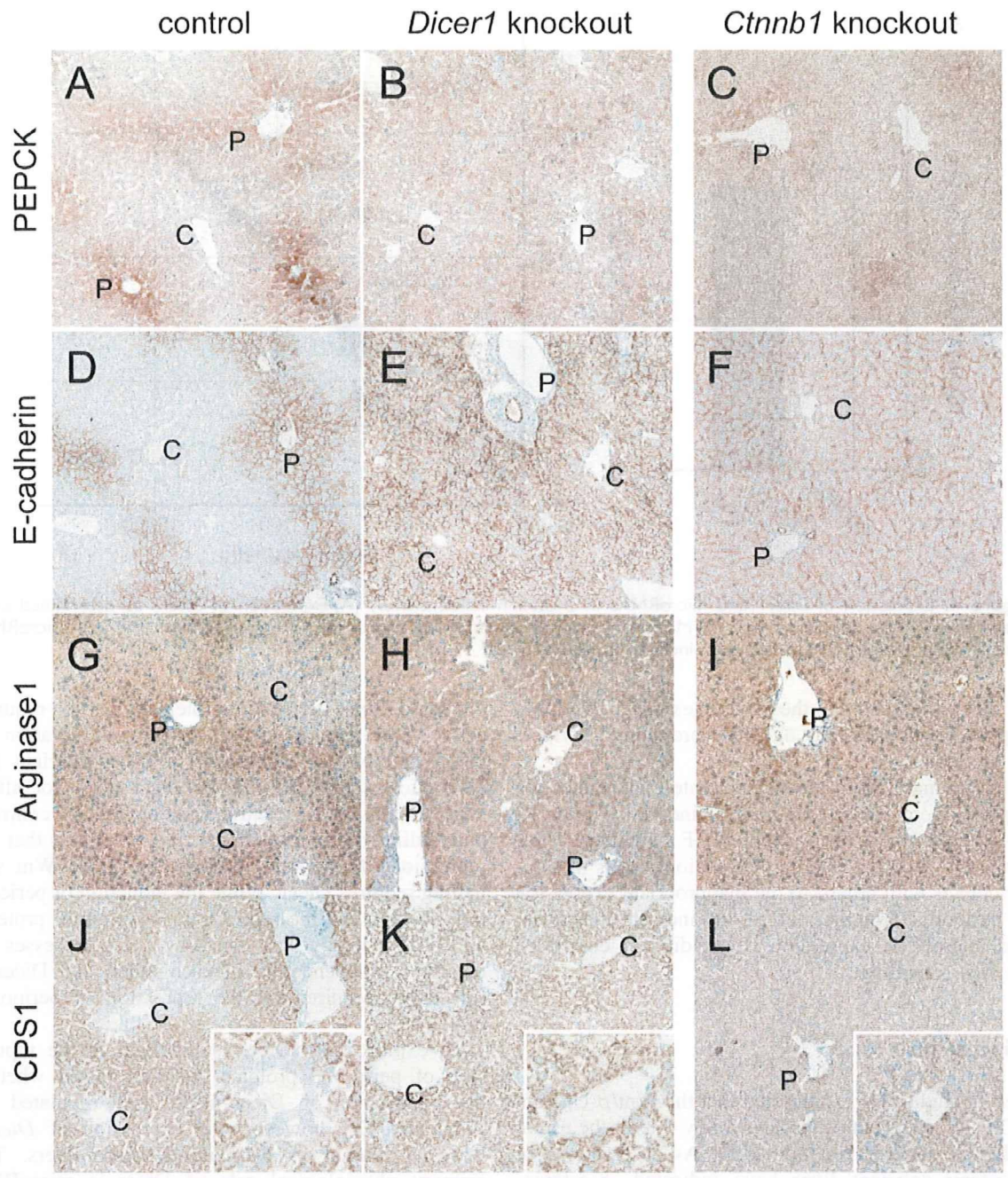

Figure 3. Expression of periportal proteins in Dicer-deficient liver. Periportal protein expression was examined using immunohistochemistry. The characteristic distributions of the periportal proteins in the control mouse liver (A, D, G, J) were completely lost in the Dicer-deficient (B, E, H, K) and β-catenin-deficient livers (C, F, I, L). High-magnification views of the pericentral areas are presented as insets for CPS1 (J–L). C = pericentral vein; P = portal tract

Dicer-deficient livers. This finding suggests that Dicer is essential for the repression of periportal proteins achieved by active Wnt signalling and that Dicer may act downstream of β-catenin/TCF. However, *Dicer1* expression was not affected in β-catenin-deficient livers, indicating that *Dicer1* itself is not involved immediately downstream of Wnt signalling (Figure 4A).

Furthermore, we performed a microarray analysis to test whether individual microRNAs are regulated by β-catenin. Similarly, a comparison of β-catenin-deficient and control livers identified no microRNAs whose expression levels were down-regulated in β-catenin-deficient livers. Thus, we did not find any microRNAs that were directly activated by β-catenin/TCF signalling (Figure 4B and Supporting information, Supplementary Table 1). On the other hand, the analysis identified four microRNAs that were up-regulated in β-catenin-deficient livers: miR-31 (2.84-fold), miR-34a (2.77-fold), miR-31* (2.91-fold), and miR-193b (2.21-fold). However, considering the modest increase

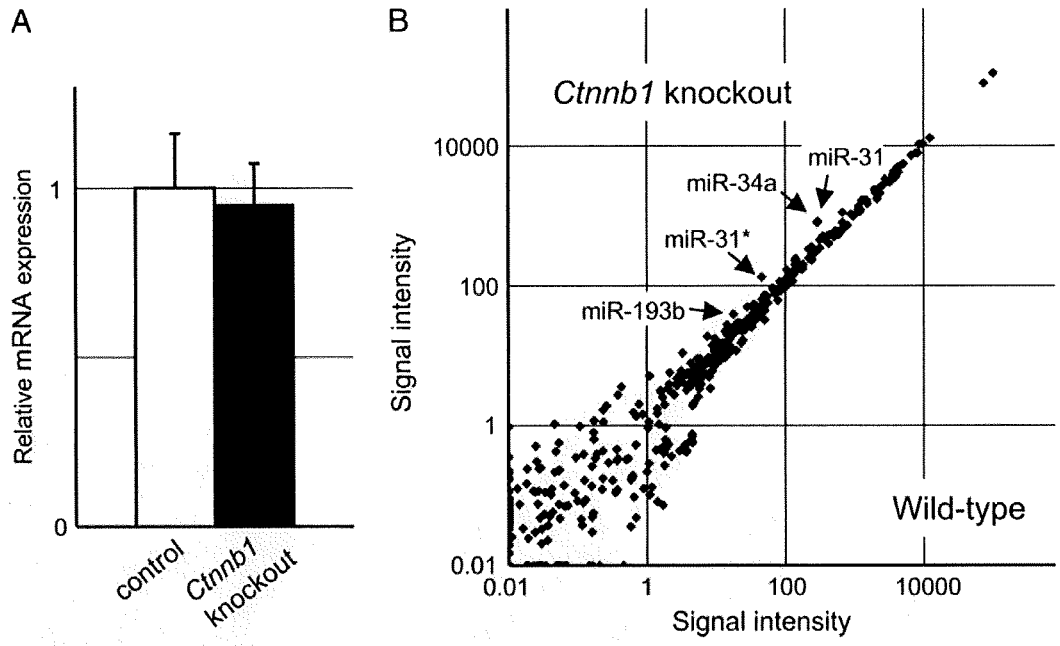

Figure 4. Expression of *Dicer1* and microRNAs in β-catenin-deficient liver. (A) Expression of *Dicer1* as determined using quantitative PCR ($n = 6$ per group). (B) Microarray analysis of microRNA expression ($n = 3$ per group). The four microRNAs with significantly altered expressions are indicated by the arrows

of these microRNAs, these changes are unlikely to explain the dramatically altered expression of periportal proteins.

In summary, our data demonstrate that neither the expression of *Dicer1* nor that of individual microRNAs is dependent on β-catenin/TCF signalling. Thus, while Dicer and β-catenin elimination results in similar defects with regard to the inappropriate expression of periportal proteins, our results indicate that Dicer and microRNA expression is not directly controlled by Wnt signalling.

Discussion

Recent studies have suggested that the Wnt/β-catenin/TCF signalling pathway plays a key role in the establishment of liver zonation [4,5]. As observations of β-catenin-deficient liver have indicated, β-catenin-mediated signalling is essential for both the expression of pericentral proteins and the repression of periportal proteins in pericentral hepatocytes. Even though MAPK signalling has been reported to affect zonation through the modulation of β-catenin/TCF-dependent transcription [11], the mechanisms underlying the establishment of zonation remain largely undefined. The present study identified Dicer as a novel and essential component in the establishment of one aspect of liver zonation, the repression of periportal proteins in pericentral areas.

The hepatocyte-specific loss of Dicer resulted in the diffuse expression of proteins that are normally localized to the periportal areas. On the other hand, the localization of pericentral proteins was left mostly unaltered. Since pericentral protein expression requires active Wnt signalling [4,8,9], the conservation of pericentral protein expression in Dicer-deficient livers indicates that the loss of Dicer does not affect Wnt activity in pericentral hepatocytes. In contrast, our findings in Dicer-deficient livers suggest that the repression of periportal proteins by active Wnt signalling requires Dicer. While the induction of pericentral proteins and the repression of periportal proteins are coordinated by Wnt signalling, these processes are regulated independently of each other, and Dicer is selectively required for the repression of periportal proteins.

To explore how Dicer is involved in the repression of periportal proteins, we first tested whether the expression of Dicer itself was regulated by β-catenin/TCF; however, the expression of *Dicer1* was not altered in β-catenin-deficient livers. The primary physiological role of Dicer is microRNA processing [12,19]. While Dicer has microRNA-independent functions, such as endogenous siRNA processing in at least some organs [20,21], Dicer's functions are generally thought to be largely mediated by microRNAs. Since microRNA precursors are mostly transcribed by RNA polymerase II [22], some microRNAs might be transactivated by β-catenin/TCF, resulting in suppression of periportal genes. Nevertheless, we could not identify any microRNAs that were down-regulated in β-catenin-deficient livers. Collectively, these observations imply that Dicer plays an essential role in the repression of periportal proteins at some point downstream of β-catenin/TCF signalling, albeit this effect likely occurs through an indirect mechanism.

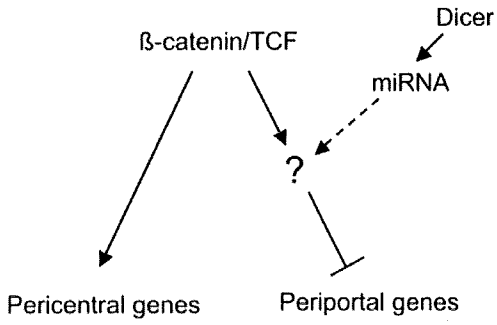

Figure 5. Model of the regulation of zonal gene expression. β-Catenin/TCF transactivates pericentral genes as well as represses periportal genes. Dicer and microRNAs are essential for the repression of periportal genes, but are not directly regulated by β-catenin

The disruption of Dicer did not have a major effect on the localization of pericentral proteins, but it did result in the expression of GS in a broader area. This finding indicates that a suppressive signal mediated by Dicer is required for the repression of GS in distal pericentral areas. A previous study reported that loss of Hnf4a also caused aberrant GS expression [23]. However, the loss of Hnf4a resulted in weak expression of GS in the entire lobule, unlike in Dicer-deficient livers, and the expression of Hnf4a was not altered in Dicer-deficient livers [18]. While the loss of Dicer and Hnf4a both affected the localization of GS, these two molecules seem to regulate GS expression through independent mechanisms.

In summary, the present study shows that Dicer is required for the establishment of proper liver zonation. Dicer is essential for the suppression of periportal proteins by Wnt/β-catenin/TCF signalling, albeit neither Dicer itself nor any individual microRNAs are directly activated by β-catenin/TCF. Our results suggest that Dicer regulates factor(s) that suppress periportal genes at some point downstream of β-catenin (Figure 5). However, the individual microRNAs responsible for the repression of periportal proteins remain elusive at present. Further studies of individual microRNAs should help to elucidate the precise mechanisms by which these factors regulate zonal gene expression in the liver.

Acknowledgements

We thank Ms Kaho Minoura (Agilent Technologies) for the microRNA analysis, Dr Magnus Ingelman-Sundberg (Karolinska Institute, Stockholm, Sweden) and Dr Masahiko Watanabe (Hokkaido University, Sapporo, Japan) for providing antibodies, and Mr Shigeru Tamura for photographic assistance. This work was supported by KAKENHI (20790315) from the Ministry of Education, Culture, Sports, Science and Technology, Japan, and a Grant-in-Aid for the Third Term Comprehensive 10-Year Strategy for Cancer Control and a Grant-in-Aid for Cancer Research from the Ministry of Health, Labour, and Welfare of Japan. Work in MH's laboratory was supported by a NIH grant (CA112537).

References

1. Jungermann K, Kietzmann T. Zonation of parenchymal and nonparenchymal metabolism in liver. *Annu Rev Nutr* 1996;**16:**179–203.
2. Gebhardt R. Metabolic zonation of the liver: regulation and implications for liver function. *Pharmacol Ther* 1992;**53:**275–354.
3. Braeuning A, Ittrich C, Kohle C, Hailfinger S, Bonin M, Buchmann A, *et al.* Differential gene expression in periportal and perivenous mouse hepatocytes. *FEBS J* 2006;**273:**5051–5061.
4. Benhamouche S, Decaens T, Godard C, Chambrey R, Rickman DS, Moinard C, *et al.* Apc tumor suppressor gene is the 'zonation-keeper' of mouse liver. *Dev Cell* 2006;**10:**759–770.
5. Hailfinger S, Jaworski M, Braeuning A, Buchmann A, Schwarz M. Zonal gene expression in murine liver: lessons from tumors. *Hepatology* 2006;**43:**407–414.
6. Gordon MD, Nusse R. Wnt signaling: multiple pathways, multiple receptors, and multiple transcription factors. *J Biol Chem* 2006;**281:**22429–22433.
7. Sekine S, Gutierrez P, Lan B, Feng S, Hebrok M. Liver specific loss of beta-catenin results in delayed hepatocyte proliferation after partial hepatectomy. *Hepatology* 2007;**45:**361–368.
8. Colnot S, Decaens T, Niwa-Kawakita M, Godard C, Hamard G, Kahn A, *et al.* Liver-targeted disruption of Apc in mice activates beta-catenin signaling and leads to hepatocellular carcinomas. *Proc Natl Acad Sci U S A* 2004;**101:**17216–17221.
9. Sekine S, Lan BY, Bedolli M, Feng S, Hebrok M. Liver-specific loss of beta-catenin blocks glutamine synthesis pathway activity and cytochrome p450 expression in mice. *Hepatology* 2006;**43:**817–825.
10. Braeuning A, Ittrich C, Koehle C, Buchmann A, Schwarz M. Zonal gene expression in mouse liver resembles expression patterns of Ha-ras and {beta}-catenin mutated hepatomas. *Drug Metab Dispos* 2007;**35:**503–507.
11. Braeuning A, Menzel M, Kleinschnitz EM, Harada N, Tamai Y, Kohle C, *et al.* Serum components and activated Ha-ras antagonize expression of perivenous marker genes stimulated by beta-catenin signaling in mouse hepatocytes. *FEBS J* 2007;**274:**4766–4777.
12. Harfe BD, McManus MT, Mansfield JH, Hornstein E, Tabin CJ. The RNaseIII enzyme Dicer is required for morphogenesis but not patterning of the vertebrate limb. *Proc Natl Acad Sci U S A* 2005;**102:**10898–10903.
13. Murchison EP, Partridge JF, Tam OH, Cheloufi S, Hannon GJ. Characterization of Dicer-deficient murine embryonic stem cells. *Proc Natl Acad Sci U S A* 2005;**102:**12135–12140.
14. Kanellopoulou C, Muljo SA, Kung AL, Ganesan S, Drapkin R, Jenuwein T, *et al.* Dicer-deficient mouse embryonic stem cells are defective in differentiation and centromeric silencing. *Genes Dev* 2005;**19:**489–501.
15. Postic C, Shiota M, Niswender KD, Jetton TL, Chen Y, Moates JM, *et al.* Dual roles for glucokinase in glucose homeostasis as determined by liver and pancreatic beta cell-specific gene knock-outs using Cre recombinase. *J Biol Chem* 1999;**274:**305–315.
16. Postic C, Magnuson MA. DNA excision in liver by an albumin-Cre transgene occurs progressively with age. *Genesis* 2000;**26:**149–150.
17. Brault V, Moore R, Kutsch S, Ishibashi M, Rowitch DH, McMahon AP, *et al.* Inactivation of the beta-catenin gene by Wnt1-Cre-mediated deletion results in dramatic brain malformation and failure of craniofacial development. *Development* 2001;**128:**1253–1264.
18. Sekine S, Ogawa R, Ito R, Hiraoka N, McManus MT, Kanai Y, *et al.* Disruption of Dicer1 induces dysregulated fetal gene expression and promotes hepatocarcinogenesis. *Gastroenterology* 2009;**136:**2304–2315.
19. Calabrese JM, Seila AC, Yeo GW, Sharp PA. RNA sequence analysis defines Dicer's role in mouse embryonic stem cells. *Proc Natl Acad Sci U S A* 2007;**104:**18097–18102.
20. Tam OH, Aravin AA, Stein P, Girard A, Murchison EP, Cheloufi S, *et al.* Pseudogene-derived small interfering RNAs regulate gene expression in mouse oocytes. *Nature* 2008;**453:**534–538.